Terahertz metamaterials with semiconductor split-ring resonators for magnetostatic tunability

Jiaguang Han,[1] Akhlesh Lakhtakia,[2] and Cheng-Wei Qiu[3,*]

[1]*Department of Physics, National University of Singapore, 2 Science Drive 3, Singapore 117542, Singapore*
Email Address: phyhanj@nus.edu.sg
[2]*Department of Physics, Indian Institute of Technology Kanpur, Kanpur 208016, India*
and
Department of Engineering Science and Mechanics, Pennsylvania State University, University Park,
PA 16802, USA (permanent address). Email Address: akhlesh@psu.edu
[3] *Department of Electrical and Computer Engineering, National University of Singapore, 4 Engineering Drive 3,*
Singapore 117576, Singapore
[*]*Corresponding author: eleqc@nus.edu.sg*

Abstract: We studied a metasurface constituted as a periodic array of semiconductor split-ring resonators. The resonance frequencies of the metasurface excited by normally incident light were found to be continuously tunable in the terahertz regime through an external magnetostatic field of suitable orientation. As such metasurfaces can be assembled into 3D metamaterials, the foregoing conclusion also applies to metamaterials comprising semiconductor split-ring resonators.

References

1. A. Lakhtakia, M. W. McCall and W. S. Weiglhofer, "Brief overview of recent developments on negative phase-velocity mediums (alias left-handed materials)," *AEÜ Int. J. Electron. Commun.* **56**, 407–410 (2002)..
2. S. A. Ramakrishna, "Physics of negative refractive index materials," *Rep. Prog. Phys.* **68**, 449–521 (2005).
3. V. M. Shalaev, "Optical negative-index materials," *Nature Photon.* **1**, 41-48 (2007).
4. *Negative Refraction Metamaterials: Fundamental Principles and Applications*, edited by G. V. Eleftheriades and K. G. Balmain (Wiley, Hoboken, NJ, USA, 2005).
5. C. Caloz and T. Itoh, Electromagnetic Metamaterials: Transmission Line Theory and Microwave Applications (Wiley, Hoboken, NJ, USA, 2006).
6. Z. Liu, H. Lee, Y. Xiong, C. Sun, and X. Zhang, "Far-field optical hyperlens magnifying sub-diffraction-limited objects," *Science* **315**, 1686 (2007).
7. D. Schurig, J. J. Mock, B. J. Justice, S. A. Cummer, J. B. Pendry, A. F. Starr, and D. R. Smith, **"**Metamaterial electromagnetic cloak at microwave frequencies,**"** *Science* **314**, 977–980 (2006)
8. T. H. Hand and S. A. Cummer, "Frequency tunable electromagnetic metamaterial using ferroelectric loaded split rings," *J. Appl. Phys.* **103**, 066105 (2008).
9. Q. Zhao, L. Kang, B. Du, B. Li, J. Zhou, H. Tang, X. Liang, and B. Zhang, "Electrically tunable negative permeability metamaterials based on nematic liquid crystals," *Appl. Phys. Lett.* **90**, 011112 (2007).
10. H.-T. Chen, W. J. Padilla, J. M. O. Zide, A. C. Gossard, A. J. Taylor, and R. D. Averitt, "Active terahertz metamaterial devices," *Nature* **444**, 579–600 (2006).
11. Y. He, P. He, V. G. Harris, and C. Vittoria, "Role of ferrites in negative index metamaterials," *IEEE Trans. Magn.* **42**, 2852–2854 (2006).
12. L. Kang, Q. Zhao, H. Zhao, and J. Zhou, "Magnetically tunable negative permeability metamaterial composed by split ring resonators and ferrite rods," *Opt. Express* **16**, 8825–8834 (2008).
13. A. Degiron, J. J. Mock, and D. R. Smith, "Modulating and tuning the response of metamaterials at the unit cell level," *Opt. Express* **15**, 1115–1127 (2007).
14. M. Lapine and S. A. Tretyakov, "Contemporary notes on metamaterials," *IET Microw. Antennas Propag.* **1**, 3–11 (2007).
15. *Polaritons: Proceedings of the First Taormina Research Conference on the Structure of Matter,* edited by E. Burstein and F. De Martini (Pergamon, New York, NY, USA, 1974).
16. *Semiconductors: Physics of Group IV Elements and III-V Compounds*, edited by O. Madelung (Springer, Berlin, Germany, 1982).

17. C. Rockstuhl, T. Zentgraf, E. Pshenay-Severin, J. Petschulat, A. Chipouline, J. Kuhl, T. Pertsch, H. Giessen, and F. Lederer, "The origin of magnetic polarizability in metamaterials at optical frequencies – an electrodynamic approach," *Opt. Express* **15**, 8871–8883 (2007).
18. N. Miura, *Physics of Semiconductors in High Magnetic Fields* (Oxford University Press, Oxford, United Kingdom, 2008).

1. Introduction

Negatively refracting metamaterials have been a subject of recent enormous interest, in both the physics and the engineering communities, because they possess electromagnetic response characteristics that are not (at least, widely) displayed by natural materials [1-3]. Generally, these metamaterials are composite materials comprising metallic inclusions of specific shapes and sizes immersed in some homogeneous host medium, and convey the promise of a wide-ranging set of applications.

Metamaterial-based devices could come to include filters, modulators, amplifiers, transistors, resonators, sub-diffraction-limited superlenses, and cloaks [4-7]. The usefulness of such a device could be extended tremendously if the metamaterial's response characteristics can be dynamically tuned. Tunability strategies examined thus far are electrical control [8-10], magnetostatic control [11,12], and optical pumping [13]. In all of cited publications, the inclusions are split-ring resonators (SRRs) made of some metal. Tunability is introduced by ensuring that another component (e.g., the substrate on which the SRRs are printed or another type of inclusions) is made of an electro-optic material, liquid crystal, ferrite, etc.

In this letter, we suggest a new type of tunable metamaterials. A metamaterial of this type comprises SRRs that are not metallic but, instead, are made of a material whose electromagnetic response properties can be tuned by an external agent. For the sake of illustration, we chose to focus on a tunable, terahertz, metamaterial that is controllable by an externally applied magnetostatic (or quasi-magnetostatic) field.

2. Analysis and numerical results

The essence of the chosen metamaterial is a metasurface [14]: a planar array of semiconductor split-ring resonators (SRRs) periodically printed on an isotropic dielectric substrate. Figure 1(a) shows a single SRR with linear dimensions in the plane ranging from 2 μm to 36 μm, and with a thickness of 200 nm. The SRRs are printed, as shown in Fig. 1(b), on a square lattice of period 60 μm. The SRRs are assumed to be made of a doped semiconductor, such as InAs, whose relative permittivity obeys the Drude model in the absence of an externally applied magnetostatic field [15,16]. As a typical isotropic dielectric substrate would only slightly shift the resonances but not affect other characteristics significantly [17], we set its electromagnetic properties to be that of free space (i.e., vacuum) in our numerical work.

Computer simulations of the spectral response of the chosen metasurface were performed using the commercial software CST Microwave Studio TM 2006B, which is a 3D full-wave solver that employs the finite integration technique. The planar SRR array was taken to be entirely surrounded by air and open boundary conditions were employed along the propagation direction. Without the applied magnetostatic field, the doped semiconductor's relative permittivity scalar ε is given as a function of the angular frequency ω by

$$\varepsilon(\omega) = \varepsilon_{\infty} - \frac{\omega_p^2}{(\omega^2 + i\gamma\omega)}, \qquad (1)$$

where ε_{∞} represents the high-frequency value; the plasma frequency $\omega_p = \sqrt{Ne^2/\varepsilon_0 m^*}$ depends on the carrier density N, the effective mass m^*, the electronic charge e, and the free-space permittivity ε_0; and γ is the damping constant. The following parameters were

used in our simulations [15,16]: $\varepsilon_\infty = 16.3$, $N = 1.04 \times 10^{17}$ cm^{-3}, $m^* = 0.004\, m_e$, and $\gamma / 2\pi = 7.5 \times 10^{11}$ Hz, where m_e is the electronic mass.
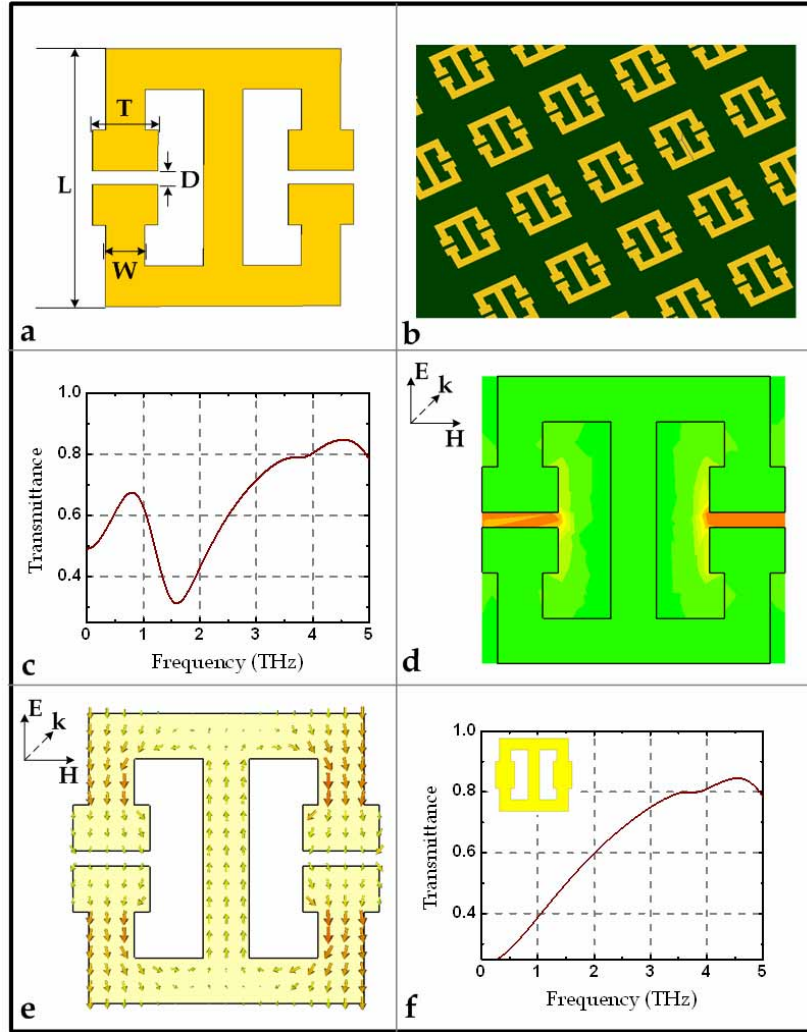

Fig. 1. (a) A single SRR with dimensions L = 36 μm, T = 10 μm, D = 2 μm and W = 6 μm. (b) The chosen metasurface, which is a square array of SRRs printed on a substrate with a period of 60 μm. (c) Transmittance spectrum of the chosen metasurface illuminated normally by a plane wave with electric field oriented perpendicular to the gaps in the SRR. (d) Map of the magnitude of the electric field in an SRR at 1.59 THz. (e) Map of the current density in an SRR at 1.59 THz. (f) The same as (c) but when both gaps are closed in every SRR.

Let the chosen metasurface be oriented parallel the *xy* plane with the two gaps of every SRR aligned parallel to the *x* axis. The SRR gaps would resonate if the incident electric field were to be oriented along the *y* axis (i.e., perpendicular to the two gaps in each SRR).

We calculated the transmittance spectrum of the metasurface when illuminated by a plane wave with its wave vector oriented parallel to the *z* axis and its electric field oriented parallel to the *y* axis. The transmittance is the ratio of the power density of the transmitted plane wave to that of the incident plane wave. Figure 1(c) shows that a transmittance dip exists at 1.59 THz frequency. This dip can be attributed to a resonance of the SRRs: as shown in Fig. 1(d),

the electric field is concentrated in both gaps of every SRR at this frequency. Figure 1(e) displays the vector plot of the current density at 1.59 THz. If both gaps of every SRR were closed, the transmittance dip at 1.59 THz would disappear, as can be gathered from the transmittance spectrum presented in Fig. 1(f).

In order to obtain a tunable response from the chosen metasurface, we considered the application of an external magnetostatic field B_0 to affect the resonance in the transmittance spectrum displayed in Fig. 1(c). Generally, without the applied magnetostatic field, the dielectric response of a semiconductor is described by a scalar $\varepsilon(\omega)$, such as provided in Eq. (1). However, when B_0 is applied, the scalar $\varepsilon(\omega)$ has to be replaced by the tensor $\hat{\varepsilon}(\omega)$.

In the Faraday configuration, B_0 is aligned parallel to the wave vector of the incident plane wave (i.e., along the z axis). With the assumption that B_0 is spatially uniform, the nonvanishing components of $\hat{\varepsilon}(\omega)$ are [15]:

$$\varepsilon_{xx} = \varepsilon_{yy} = \varepsilon_\infty - \frac{\omega_p^2(\omega^2 + i\gamma\omega)}{(\omega^2 + i\gamma\omega)^2 - \omega^2\omega_c^2}, \qquad (2)$$

$$\varepsilon_{xy} = -\varepsilon_{yx} = i\frac{\omega\omega_c\omega_p^2}{(\omega^2 + i\gamma\omega)^2 - \omega^2\omega_c^2}, \qquad (3)$$

$$\varepsilon_{zz} = \varepsilon_\infty - \frac{\omega_p^2}{(\omega^2 + i\gamma\omega)}, \qquad (4)$$

where $\omega_c = eB_0/m^*$ is the cyclotron frequency. The off-diagonal components ε_{xy} and ε_{yx} are induced by the magnetostatic field and depend on its magnitude. Figure 2(a) contains the simulated transmittance spectra of the chosen metasurface for different values of the magnitude B_0 of B_0. The transmittance dip redshifts gradually from 1.55 to 0.30 THz as B_0 is increased from 1.0 to 8.0 T, as also illustrated in Fig. 2(b). Although the minimum transmittance increases as B_0 is increased, Figs. 2(a) and 2(b) clearly indicate that planar arrays of semiconductor SRRs are magnetically tunable in the terahertz regime despite the reduction of the quality factor of the transmittance dip. The reduction of the quality factor and the use of very-high-magnitude magnetostatic fields in the presented results suggest the need to find and/or develop semiconductors that respond more easily to magnetostatic fields.
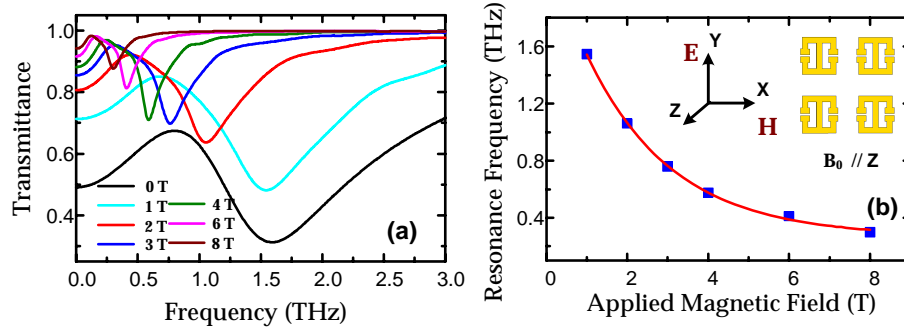

Fig. 2. Faraday configuration. (a) Transmittance spectra for various values of B_0, when B_0 is aligned parallel to the wave vector of the incident plane wave and the electric field of the incident plane wave is aligned perpendicular to the gaps in each SRR. (b) Resonance frequency ω_0 as a function of B_0, with the solid line showing the exponential fit $\omega_0 = \alpha + \beta\exp(-B_0/\chi)$, where $\alpha = 0.27$, $\beta = 2.04$, and $\chi = 2.11$.

Denoting the resonance angular frequency by ω_0, we fitted the data in Fig. 2(b) to the formula $\omega_0 = 0.27 + 2.04 \exp(-B_0/2.11)$. This formula indicates that the resonance frequency decays exponentially as the applied magnetostatic field increases in magnitude. One way to understand the foregoing trend is as follows. In the Faraday configuration, plane wave propagation in a semiconductor depends on [18], i.e., $\varepsilon_{\pm} = \varepsilon_{xx} \pm i\varepsilon_{xy} = \varepsilon_{\infty} - \dfrac{\omega_p^{2}}{\omega^2 + i\gamma\omega \mp \omega\omega_c}$.

Let $\tilde{n}_{\pm}^{2} = \varepsilon_{\pm}$, where $\tilde{n}_{+}$ and $\tilde{n}_{-}$ are the complex-valued refractive indexes for right- and left-circularly polarized plane waves. For the linearly polarized electromagnetic wave in our case, the response of substance can be captured by $\tilde{n} = \dfrac{1}{2}(\tilde{n}_{+} + \tilde{n}_{-})$ for different values of B_0. As shown in Fig. 3, the real part of $\tilde{n}$ decreases as B_0 increases. So the redshift of ω_0 with increase of B_0 can be correlated with the concurrent decrease of $\tilde{n}$.
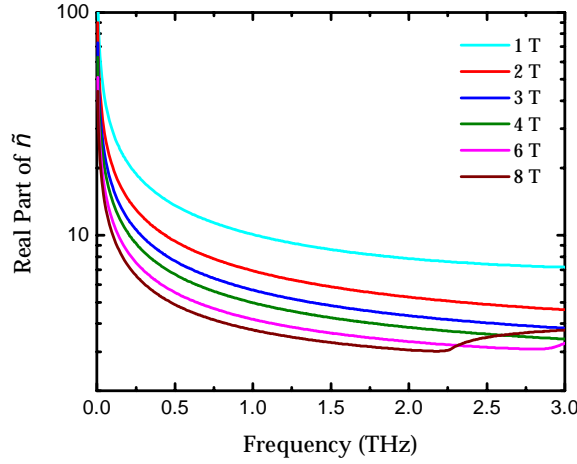

Fig. 3. Real part of $\tilde{n}$ as a function of the linear frequency $\omega/2\pi$ and the magnitude B_0 of the applied magnetostatic field in the Faraday configuration.

So far we have considered the Faraday configuration. In the Voigt configuration, the magnetostatic field is aligned perpendicular to the wave vector of the incident plane wave. There are two cases, depending on the direction of the incident electric field relative to $\boldsymbol{B_0}$. Suppose first that $\boldsymbol{B_0}$ is also aligned perpendicular to the electric field of the incident plane wave (i.e., $\boldsymbol{B_0}$ is oriented along the x axis). The nonvanishing components of $\hat{\varepsilon}(\omega)$ now are [15]

$$\varepsilon_{yy} = \varepsilon_{zz} = \varepsilon_{\infty} - \frac{\omega_p^{2}(\omega^2 + i\gamma\omega)}{(\omega^2 + i\gamma\omega)^2 - \omega^2\omega_c^{2}}, \qquad (5)$$

$$\varepsilon_{yz} = -\varepsilon_{zy} = i\frac{\omega\omega_c\omega_p^{2}}{(\omega^2 + i\gamma\omega)^2 - \omega^2\omega_c^{2}}, \qquad (6)$$

$$\varepsilon_{xx} = \varepsilon_{\infty} - \frac{\omega_p^{2}}{(\omega^2 + i\gamma\omega)}. \qquad (7)$$

Figure 4(a) shows that the transmittance spectra in the first Voigt configuration are qualitatively similar to that for the Faraday configuration in Fig. 2(a). The resonance frequency exponentially redshifts as B_0 increases, and can be fitted to

$\omega_0 = 0.27 + 1.64 \exp(-B_0/3.03)$; see Fig. 4(b). Furthermore, in this configuration, the electromagnetic response of the semiconductor is related to $\tilde{n}_\perp = (\varepsilon_{yy} + \varepsilon_{yz}^2/\varepsilon_{yy})^{1/2}$. Figure 5 shows that real part of $\tilde{n}_\perp$ decreases with increasing B_0, which implies the same correlation with the resonance frequency as deduced for the Faraday configuration.
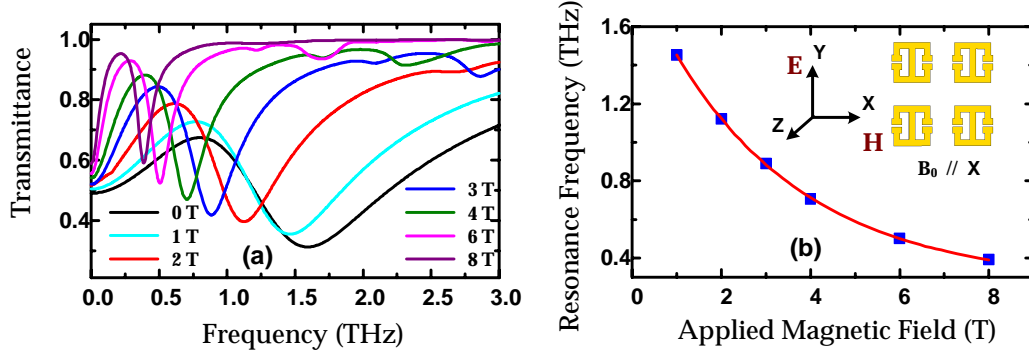

Fig. 4. First Voigt configuration. (a) Transmittance spectra for various values of B_0, when $\boldsymbol{B_0}$ is aligned parallel to the gaps in each SRR and the electric field of the incident plane wave is aligned perpendicular to the gaps in each SRR. (b) Resonance frequency ω_0 as a function of B_0, with the solid line showing the exponential fit $\omega_0 = \alpha + \beta \exp(-B_0/\chi)$, where $\alpha = 0.27$, $\beta = 1.64$, and $\chi = 3.03$.
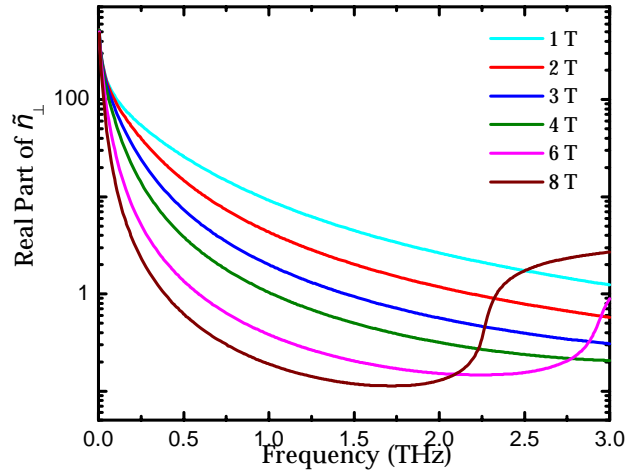

Fig. 5. Real part of $\tilde{n}_\perp$ as a function of the linear frequency $\omega/2\pi$ and the magnitude B_0 of the applied magnetostatic field in the first Voigt configuration.

In the second Voigt configuration, $\boldsymbol{B_0}$ is aligned parallel to the electric field of the incident plane wave (i.e., $\boldsymbol{B_0}$ is oriented along the y axis), so that the nonvanishing components of $\hat{\varepsilon}(\omega)$ now are [15]

$$\varepsilon_{xx} = \varepsilon_{zz} = \varepsilon_{\infty} - \frac{\omega_p^2 (\omega^2 + i\gamma\omega)}{(\omega^2 + i\gamma\omega)^2 - \omega^2 \omega_c^2}, \tag{8}$$

$$\varepsilon_{zx} = -\varepsilon_{xz} = i \frac{\omega\omega_c \omega_p^2}{(\omega^2 + i\gamma\omega)^2 - \omega^2 \omega_c^2}, \tag{9}$$

$$\varepsilon_{yy} = \varepsilon_{\infty} - \frac{\omega_p^2}{(\omega^2 + i\gamma\omega)}. \tag{10}$$

We found that there is no remarkable effect of the applied magnetostatic field on the resonance frequency of the chosen metasurface; furthermore, the electromagnetic response of the semiconductor is related to $\tilde{n}_{//} = \varepsilon_{yy}^{1/2}$, which does not depend on B_0.

3. Conclusion

To conclude, our computer simulations have shown that the terahertz resonant response of a metasurface constituted by a planar array of semiconducting split-ring resonators can be tuned by the application of an externally applied magnetostatic field of appropriate orientation and magnitude. As such metasurfaces can be assembled into 3D metamaterials, the foregoing conclusion applies to metamaterials comprising semiconducting SRRs as well. SRRs made of other tunable materials, such as electro-optic materials, could also assist in the realization of tunable terahertz metamaterials.

Acknowledgements